THE JOURNAL OF PHYSICAL CHEMISTRY C

Article

pubs.acs.org/JPCC

Combined W-Band Light-Induced ESR/ENDOR/TRIPLE and DFT Study of PPVtype/$PC_{61}BM$ Ion Radicals

Alexander Konkin,[*,†] Alexey Popov,[‡] Uwe. Ritter,[†] Sergei Orlinskii,[§] Georgy Mamin,[§] Albert Aganov,[§] Aleksei A. Konkin,[†,§] and Peter Scharff[†]

[†]Institute of Micro- and Nanotechnologies MacroNano, Technische Universität Ilmenau, Gustav-Kirchhoff- Str.7, D-98693 Ilmenau, Germany

[‡]Leibniz Institute for Solid State and Materials Research, IFW Dresden, Helmholtzstraße 20, 01069 Dresden, Germany

[§]Institute of Physics, Kazan Federal University, Kremlyovskaya Str. 18, Kazan, Russia

Supporting Information

ABSTRACT: The combined W-band pulsed light-induced multiresonance ESR/ENDOR/TRIPLE technique and DFT calculation have been applied to study the ^1H hyperfine coupling and electron spin density distribution on PPV cation and $PC_{61}BM$ anion radicals in (PPVs):$PC_{61}BM$ blends. The sign of calculated electron spin density populations of protons delocalized on polymer and fullerene side chain has been confirmed experimentally by means of TRIPLE in frozen solution at the temperature of 20 K.

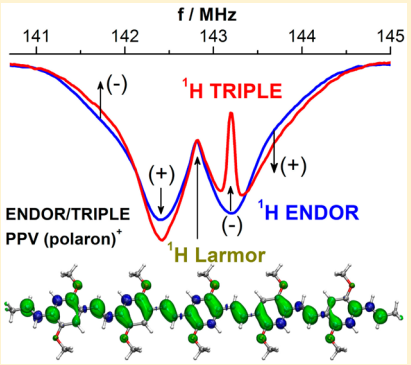

1. INTRODUCTION

While the evident progress of power conversion efficiency (PCE) increase of organic solar cells (OSC) during the past decade is observed definitely[1] and as expected will achieve soon the commercialization, some fundamental aspects of the charge distribution of ion radicals formed under the light excitation in OSC electron donor/acceptor blends are not clear yet. Light induced electron spin resonance (LESR) and appropriate magnetic multiresonance methods applied to the OSC study may be considered as an efficient method in this field due to the direct attribution of the detected number of ion radical spins to the number of charges generated in the photoelectron transfer process. Among the numerous ESR applications to OSC composites, studies of the hyperfine coupling (hfc) of electron−nuclear spins in photogenerated ion radicals plays a special role. Experimental hfc data on ion radicals in donor/acceptor OSC blends can be considered as the basic technique for determination of the spin density distribution (SDD) in electron donor and acceptor molecules. For the majority of ion radicals in conjugated polymer/fullerene blends the hyperfine structure cannot be resolved by continuous-wave (CW) ESR due to small hfc values. However, electron nuclear double resonance (ENDOR) can partially overcome this problem as was already demonstrated by the evaluation of hfc parameters for OSC blends,[2,3] as well as for undoped and doped conjugated polymers.[4a−c,5] For the polymer photoelectron donors, ENDOR allows validation of the density functional theory (DFT) calculations, in particular to estimate delocalization length of the photoinduced polaron on the polymer chain. Such experiments are important for the estimation of intrinsic quantum efficiency (IQE) of polymers. Precise ENDOR determination of SDD along the oligomer chains has been demonstrated in PTB7, PTDTBT polymer photoelectron donors blended with $PC_{70}BM$ as electron acceptor.[2] The registered ENDOR frequencies of polarons in PTB7, PTDTBT oligomers (n-monomers) with the different n gives SDD of photoinduced polaron on polymer chain, i.e., the limit of polaron delocalization expansion due to its coincidence with the ENDOR data in appropriate oligomers. For instance, the information concerning the decrease of polaron delocalization length in PTB7 and PTDTBT in comparison with P3HT correlates with increase of the short circuit current density (I_{SC}) in OSC that can be attributed, at least partly, to appropriate increase of the number of photoinduced polarons. However, in the model oligomer SDD calculation and its comparison with experimental ENDOR data, the opportunity of the side chain influence to SDD delocalization has not been considered so far. While the use of abridged side chains in oligomers in computational studies is usually justified by to the dramatic increase of calculation procedure time, their accounting at least with the simplified appropriate chemical structure of the side chain could be important in order to estimate their contribution

Received: August 9, 2016
Revised: October 29, 2016
Published: November 28, 2016

DOI: 10.1021/acs.jpcc.6b08034
J. Phys. Chem. C 2016, 120, 28905−28911

to the ligand hyperfine interaction by ENDOR. This equally relates to the fullerene derivatives (FD). With respect to FD with the side chains including only C and H atoms, the data of ^{1}H ENDOR could be considered as a spin label for the SDD detection on carbons in side chain for instance via McConell equation for hfc parameters. In the case of a good correlation between ^{1}H ENDOR and DFT data, one can expect the validity of computed SDD on fullerene frame obtained by DFT calculation. The delocalization of SDD, or in case of ion radical noncompensated charge distribution on fullerene frame, can play a role for the electron transport in acceptor medium. For instance, the essential inhomogeneous of SDD on FD frame in some isomers of $PC_{70}BM$ anion radical obtained by DFT was reported in the literature,[6] and the influences of such inhomogeneity on the electron hopping (activation energy barrier) between FD molecules should be under the additional consideration. Therefore, an application of ^{1}H ENDOR/TRIPLE (electron−nuclear−nuclear triple) for the electron spin density relocation study on anion radicals between fullerene frame and its side chain in modified fullerenes as well as its influence on the electron transport can be considered important.

2. EXPERIMENTAL SECTION

The [6,6]-phenyl C61 butyric acid methyl ester ($PC_{61}BM$) was purchased from Aldrich, and M3EH-PPV (below is denominated as P2) was provided by D. A. M Egbe,[7] and their chemical structures are shown in Figure 1. P2:$PC_{61}BM$ blend

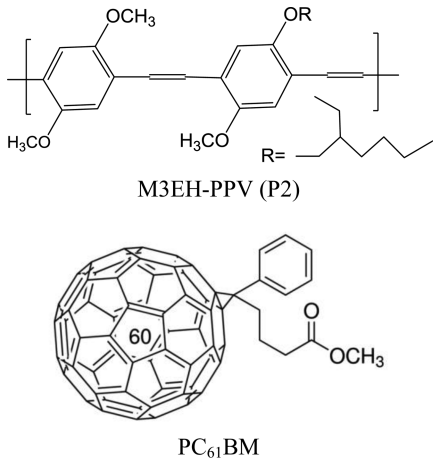

Figure 1. M3EH-PPV (P2) and $PC_{61}BM$ structure.

was combined with a weight ratio (w.r.) of 1:1 and diluted in dichlorobenzene under ultrasonic condition during 20 min. The above solution was used in LESR experiments at 20 K temperature. The electron spin echo (ESE) detected W-band (94 GHz) light induced ESR (below in text will be denominated as W-band LESR), Mims ENDOR (below in text ENDOR only), and TRIPLE spectra were recorded using a Bruker BioSpin multiresonance spectrometer ELEXYS E680. Mims ENDOR and TRIPLE experiments were done using the microwave scheme $\pi/2-\tau-\pi/2-T-\pi/2-\tau-$echo with one (ENDOR) or two (TRIPLE) π rf pulses applied for time T = 160 μs with $t(p/2)$ = 20 ns and t(rf) = 78 μs. An accumulation of 2048 to 16384 scans was sufficient to obtain an acceptable signal-to-noise ratio. A repetition time of 3 ms and τ value of 288 ns were used. The illumination has been provided by the optical fiber from a diode-laser (532 nm) with the 50 mW output power.

Optimization of molecular structures of $PC_{61}BM$ and polymer oligomers was performed at the PBE/TZ2P level using Priroda code.[8,9] Hyperfine coupling constants were then computed in Orca suite[10] at the B3LYP/6-311G* level with the use of specially tailored EPR-III basis set for protons. Spin density distributions were visualized with VMD.[11]

3. RESULTS AND DISCUSSION

3.1. P2:$PC_{61}BM$. W-Band ESR/ENDOR Spectra. While the application of X-band ENDOR technique has been successfully used in polaron ligand hfc study in conjugated polymers some important information concerning ligand proton interactions in anion radicals of fullerene derivatives can be lost due to overlap of ESR signals of polaron and fullerene anion in X,K,Q-bands ESR spectra and therefore resulting overlap of appropriate ENDOR spectra around ^{1}H Larmor frequency (f_L).This obstacle can also influence on processing the results of TRIPLE measurements as will be introduced below. In such cases, W-band ESR/ENDOR technique can circumvent the problem as demonstrated in Figure 2 showing LESR and ENDOR spectra of P2-$PC_{61}BM$.

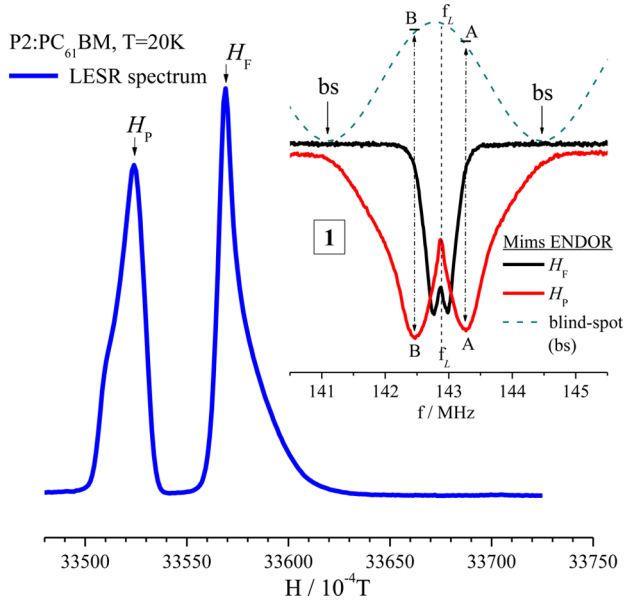

Figure 2. Light-induced (532 nm) electron spin echo detected spectrum of P2:$PC_{61}BM$ blend recorded at 20 K temperature with the denominations of field points of ENDOR registration (H_P and H_F of PPV polaron and $PC_{61}BM$ anion radical, respectively). Inset **1** shows the ENDOR spectra, recorded in appropriate H_P and H_F magnetic field points, and extracted blind sport curve explaining the insignificant asymmetry of polymer polaron ENDOR line amplitude maximums around the Larmor frequency f_L.

ENDOR spectra of both components recorded in H_P and H_F field points (Figure 2 and its insert **1**) are free from any contributions of each other due to the high resolution of W-band ESR spectra. Some difference in ENDOR spectra amplitudes (points A and B in insert **1** in Figure 2) is attributed to the insignificant displacement of the blind-spot curve maximum relatively Larmor frequency.

3.2. Combined DFT and ENDOR/TRIPLE Results. *3.2.1. M3EH-PPV (P2).* Theoretical SDD and ENDOR study

DOI: 10.1021/acs.jpcc.6b08034
J. Phys. Chem. C 2016, 120, 28905−28911

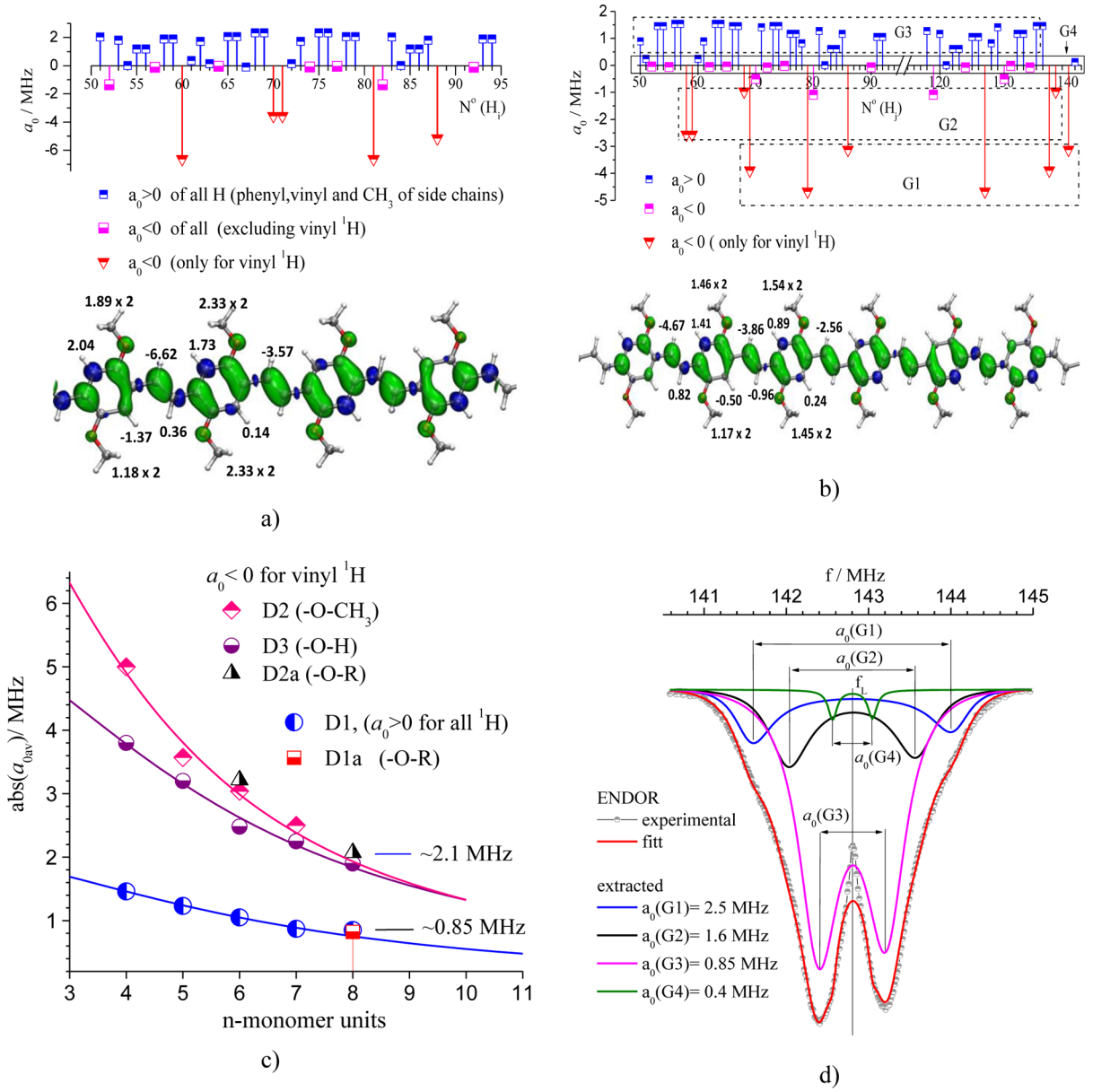

Figure 3. (a,b) ^{1}H isotropic hfc constant (a_0) calculated for PPV 4- and 6- oligomers with −O−CH_3 side chains; the ascription of appropriate C,O,H oligomer atoms in polymer and side chains for 4- and 6- oligomers in expanded scale are exhibited in SI-1a,b). (b) One of the possible versions of a_0 group assignment, which is suitable for the ENDOR experimental spectrum simulation in (Figure 3d. (c) Average in groups abs(a_{0av}) dependence from the number of monomer units: D1, the data corresponded to all protons, i.e., phenyl, vinyl, and − O−CH_3 of side chains excluding values of vinyl ^{1}H with a_{0ev} < 0; D2, vinyl ^{1}H with a_{0ev} < 0 calculated for 4-, 5-, 6-, 7-oligomers with −O−CH_3 side chain; D3, vinyl ^{1}H with a_{0ev} < 0 calculated for the 4- and 8-oligomers with the −O−H side chain; D1a and D2a, DFT data corresponding to oligomers with −O-R (Figure 1); solid lines are the approach of Lorentz distribution function. (d) Experimental, fitted, and extracted P2 ENDOR spectra for G1, G2, G3, and G4 groups with the appropriate a_0(G1,2,3,4) values: a_{0ev}(G1,2) ≈ (2.5 + 1.6)/2 ≈ 2.1 MHz, a_{0ev}(G3) = 0.85 MHz.

of some poly(*p*-phenylen-vinylen (PPV) derivatives is introduced in ref 4a; however, usually the side chains of oligomers are excluded from the consideration. With regard to DFT calculation of PPV oligomers, in this work the evaluation of SDD on phenyl side chain −O−CH_3 and −O−R, where R is appropriate group in P2 (Figure 1), has been included due to necessity of quantitative comparison of calculated and experimental hfc parameters obtained by means of ENDOR/TRIPLE. The preliminary monomer and dimer computations of PPV family like poly[2-methoxy-5-(3′,7′-dimethyloctyloxy)-1,4-phenylenevinylene (MDMO-PPV), poly[2-methoxy-5-(2-ethylhexyloxy)-1,4-phenylenevinylene] (MEH-PPV), and (poly[2,5-dimethoxy-1,4-phenylene-1,2-ethenylene-2-methoxy-5- (2-ethylhexyloxy)-(1,4-phenylene-1,2-ethenylene)]) M3EH-PPV show that SDDs of only the first methylene group next to oxygen in −O−R side chains of polymers (R = −CH_2−) can be taken into account, whereas further protons have vanishingly small spin populations and can be neglected. Therefore, instead of complete side chains, the simple substitution of extended R groups by −CH_3 (i.e., −O−CH_3) is sufficient for the correct evaluation of the side chain contributions to overall SD distribution in oligomers, at least with n > 8. In order to confirm the above approach the calculation of 6- and 8-oligomers with unabridged real −O−R groups has been carried

DOI: 10.1021/acs.jpcc.6b08034
J. Phys. Chem. C 2016, 120, 28905−28911

out as well, and the results are included in Figure 3c. Other DFT data for 5-, 6-, 7-, 8-oligomers with $-O-CH_3$ and $-O-R$ are introduced in SI-1. The proton isotropic hfc constants (a_0) for two oligomers (4-, 6-) are demonstrated in Figure 3a,b. These calculations show that the main feature of the SDD in oligomers is the different a_0 sign as well as absolute average values (at about 2−3 times) of phenyl and vinyl protons. These data can be considered as a suitable example for the experimental verification by means of ENDOR/TRIPLE. For the convenience of comparison with ENDOR/TRIPLE experiments, a_0 values were separated at the several groups (G1, G2, G3, and G4) combining a_0 with the approximately the same values as shown in Figure 3b and evolved by the boxed displays marked in the same manner G_j (j = 1, 2, 3, 4). For the experimental $PC_{61}BM$ ENDOR spectrum (same as in Figure 2 in inset 1), its fitting includes the set of the four ^1H group contributions as well as their separated spectra, according to the group denomination G_j, shown in Figure 3d. The reasonable fitting of ENDOR spectrum has been achieved taking into consideration mainly three (G1, G2, G3) groups responsible for the hyperfine structure. The deviation of a_0 in G_j groups is supposed due to the structure calculation in gas phase; however, in general, the definite features of a_0, i.e., relative values and signs for phenyl and vinyl groups are the same for the all calculated oligomers. The dependence of average a_0 (a_{0ev}) from the number of monomers units in oligomer is shown in Figure 3c. With regards to TRIPLE (double ENDOR) origin mainly used for hfc sign determination, the detailed consideration is widely introduced in the literature (for instance, refs 12−14), and here, only the general qualitative features of TRIPLE results are briefly introduced. In case of complete spectrum record, i.e., in both intervals $f < f_L$ and $f > f_L$ (note that for ENDOR the complete record is not necessary) the pumping at the ENDOR line with the definite sign of hfc parameter initiates the increase of its absolute amplitude in the symmetric/opposite side from f_L as well as all the other ENDOR lines attributed to the same sign of hfc. Opposite behavior of spectrum takes place in interval where this RF pumping is applied. For the ENDOR line attributed to the other sign of hf coupling one can observe the opposite result due to inversion of electron−nuclear level population for nuclear state with the other sign of hfc. The use of this technique for the system with unresolved ENDOR spectra is illustrated in Figure 4a,b. Two pumping frequencies f_1, f_2 ($|f_1 - f_L| = |f_2 - f_L| = \Delta f_a$) in TRIPLE were used in two different experiments in order to ensure the ENDOR line shape response. In Figure 4a TRIPLE with f_1, as expected, increases the ENDOR amplitude in opposite $f < f_L$ range (box B1 in Figure 4a), decreases ENDOR line amplitude in wide range, included in box A1, and increases amplitude in symmetric position in box A2. To check the opposite response of the ENDOR line, the pumping with f_2 was applied and analogous mirrored result was obtained, viz. the increase of ENDOR amplitude in box A1 and decrease in box A2 as shown in Figure 4b. All the appropriate deviations of ENDOR line amplitudes are denominated in appropriate boxes: A1, A2, B1 by arrows in Figure 4a. The additional illustration of G1, G2 groups and group G3 hfc signs difference is introduced in Figure 4c, which shows the different ENDOR-TRIPLE(f_2) spectrum and the correlation of the wide range response in TRIPLE spectra with the wide distribution or deviation of vinyl hfc parameters in G1, G2 groups. Therefore, with respect to the sign of ^1H hfc parameters in PPV fragment, the TRIPLE data are in good

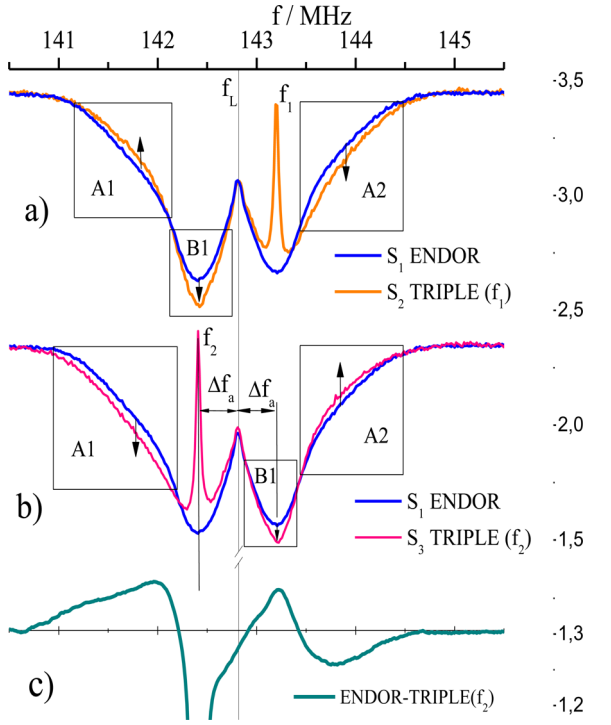

Figure 4. (a,b) polymer polaron ENDOR (S_1) and TRIPLE ($S_{2,3}$) spectra with the frequency pump at $f_{1,2} = f_L \pm \Delta f_a$. In boxes A1, A2, and B1 are shown the main deviations of ENDOR spectrum amplitude under the additional frequency pumps in TRIPLE experiment. Note that the additional, symmetric relatively Larmor frequency, f_2, pump has been performed for the guarantee of the TRIPLE response attribution, based on DFT data. (c) ENDOR-TRIPLE spectrum with f_2 pump. Amplitude scales for $S_{1,2,3}$ spectra and ENDOR-TRIPLE spectrum is shown on the right side of the figure.

agreement with the results of DFT calculations. Additionally, the absolute values of fitted a_0 of ENDOR spectra in Figure 3d, i.e., ∼2.5, ∼1.6, and ∼0.85 MHz, attributed to G1, G2. and G3 groups, respectively, correlate well with the DFT data for 8−9 monomer units as shown in Figure 3c, i.e., ∼2.1 MHz for vinyl and ∼0.8 MHz for phenyl proton groups (note that in Figure 3c for vinyl protons a_{0ev} is the average value for G1 and G2 groups, keeping in mind that their integral intensities are approximately the same). The result of 8−9 monomer units of polaron delocalization coincides with the data reported in ref 5 for MDMO-PPV. Therefore, TRIPLE experiment confirms the DFT data of PPV fragment with a good accuracy. It should be noted that the reproducibility of M3EH-PPV polaron ENODR spectrum shown in inset 1 in Figures 2 and 3d was confirmed experimentally with the several prepared M3EH-PPV:PC61MB blends diluted in *o*-DClB and the example of spectrum as well as the comments concerning the variety of spectra parameter sets are displayed in SI (SI-3).

3.2.2. $PC_{61}BM$. With respect to $PC_{61}BM$, the correlation between ENDOR and DFT data is not so perfect as in P2 and shows a deviation of a_0 ENDOR and DFT values at about two times (Figure 5). This should not be surprising taking into account that in polymers many protons are directly bonded to the carbons comprising the π-system (which bears the main SD), whereas in anion-radicals of fullerene derivatives the spin density is mainly localized on the fullerene core; besides, the side chain in $PC_{61}BM$ is subject to conformational disorder. DFT calculations of two different $PC_{61}BM$ conformers

DOI: 10.1021/acs.jpcc.6b08034
J. Phys. Chem. C 2016, 120, 28905−28911

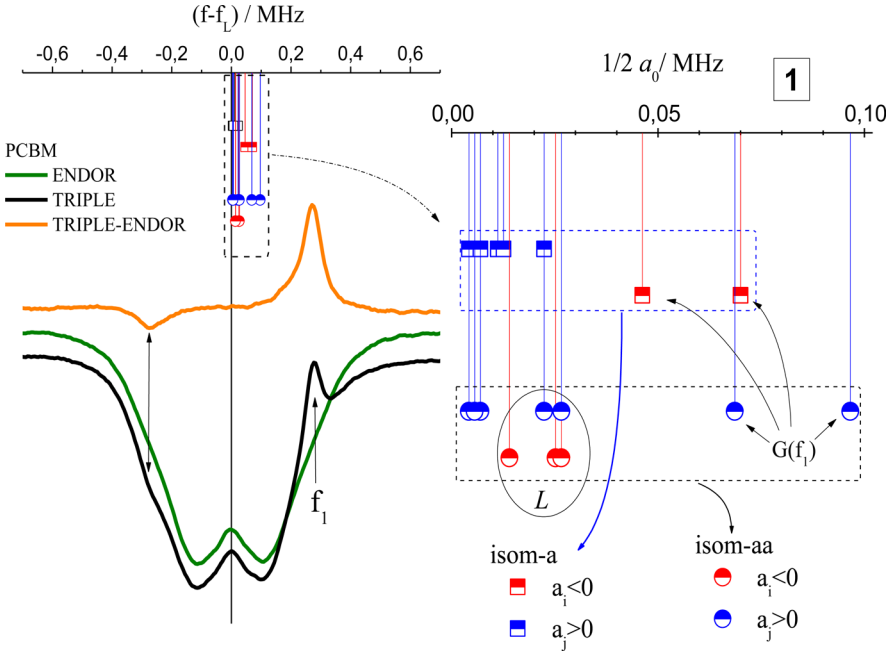

Figure 5. $PC_{61}BM$ ENDOR, TRIPLE (pump at $f_1 = f_L + 0.25$ MHz) and TRIPLE(f_2)-ENDOR spectra with DFT data of $1/2a_0$ values for two $PC_{61}BM$ isomers (arbitrary denominated as conformers -a and -aa) with energy difference of 34 kJ/mol. In inset 1 is the expanded scale of DFT results with appropriate denominations of $a_{0i,j}$ sign. G(f_1) group in inset 1 includes two ^1H with the same SD sign and is attributed to the protons displaced more from the f_L than other ones.

(denoted as isom-a and isom-aa in Figure 5, with relative energies of 34 and 0 kJ/mol, respectively, in the anionic state) found the difference in absolute values as well in sign for the same types ^1H a_0 as shown in inset 1 in Figure 5 (all the appropriate proton denominations and a_0 values are introduced (SI-2). TRIPLE with f_1 gives the expected response of ENDOR line in appropriate symmetric position on other side of f_L (TRIPLE-ENDOR spectrum in Figure 5), but not an additional information on hfc structure, at least concerning the a_0 sign in ENDOR spectrum. However, the result of radio frequency (RF) pumping at frequency f_2 introduced in Figure 6a relocates the focus of interest significantly. The change of ENDOR spectrum in opposite side of f_2 (box C1) is evident and certainly is reflected in ENDOR-(TRIPLE)x1 spectrum in Figure 6. The part of this spectrum (in box C2) supposes the response in TRIPLE spectrum for two nearby ENDOR lines with different sign of hfc constants denoted here as a_1 and a_2. It was supposed that in points $a_1/2$ and $a_2/2$ the amplitudes in ENDOR-(TRIPLE)x1 spectrum have opposite signs. This supposition was checked and confirmed by the model approach exhibited in Figure 6b, where the simulated spectra are attributed to the experimental ENDOR/TRIPLE spectra limited by the RF interval in box C1. Simplified version of two nearby lines $S_1(a_1)$ and $S_2(a_2)$ with the same amplitudes A_{a1} and A_{a2} gives resulting $S_3 = S_1 + S_2$ model ENDOR spectrum. TRIPLE transforms S_1 and S_2 to S_{11} and S_{22}, respectively, with appropriate $-A_{a1} - \Delta A_{a1}$ and $-\Delta A_{a2} + \Delta A_{a2}$ amplitudes and resulting in $S_{33} = S_{11} + S_{22}$ TRIPLE spectrum (note that for the modeling $\Delta A_{a1} = \Delta A_{a2} = 0.2A_{a1}$ has been taken). The correlation between experimental and simulated data was obtained via processing of ENDOR-(TRIPLE) × K data for both experimental and model spectra. Coefficient K (values are displayed in Figure 6) was used for the normalization of ENDOR and TRIPLE spectrum amplitudes at the same value in spectrum points corresponded to $a_1/2$ and

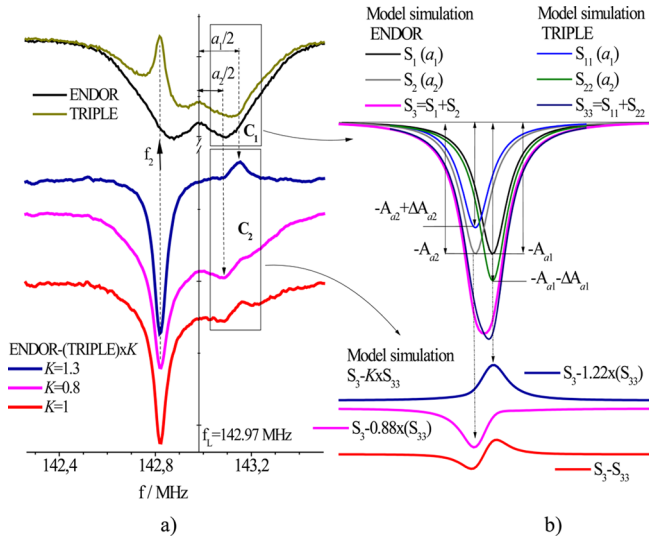

Figure 6. (a) ENDOR, TRIPLE with $f_2 = f_L - 0.15$ MHz, and ENDOR-(TRIPLE)xK spectra of $PC_{61}BM$ anion radical. Parameter × K is the normalization coefficient and used in ENDOR-(TRIPLE) × K processing that is described in detail in the text. (b) Model spectra corresponding to the nearby overlapped lines introduced in the experimental part in boxes C_1 and C_2 in panel a, with the frequency difference at about $(a_1 - a_2)/2 = 0.1$ MHz. All spectra amplitude denominations and assignment to the model spectra as well as attribution of the individual model lines to experimental ones with hfc a_1 and a_2 are shown. The appropriate detailed discussion is in text.

$a_2/2$ positions and therefore excludes one while enhancing another line in ENDOR-(TRIPLE) × K spectrum and vice versa. The resulting of ENDOR-(TRIPLE) × K model spectra in Figure 6b correlate completely with the obtained by experimental ones, shown in box C2 of Figure 6a. Returning back to inset 1 in Figure 5 one can suppose that isomer-aa is

DOI: 10.1021/acs.jpcc.6b08034
J. Phys. Chem. C 2016, 120, 28905−28911

more suitable for experimental data owing to the larger hfc values and the presence of several nearby and/or partly overlapping lines with the different sign of a_0 close to the frequency interval around $a_1/2$ and $a_2/2$ (Figure 6a). It should be also highlighted that the same procedure does not change the position of extremum in ENDOR-(TRIPLE) × K spectrum with any K values around G(f_1) group (inset 1 in Figure 5), hypothetically responsible for the TRIPLE-ENDOR spectrum part in interval $(f - f_L) < 0$ in Figure 5. The last confirms the absence of nearby lines with opposite a_0 sign and correlates with the data predicted for the isomer-aa in line with its higher thermodynamic stability. Keeping in mind the relatively weak TRIPLE response relatively ENDOR spectra amplitude for the both ion radicals one can suppose the low probability of surely TRIPLE spectrum detection at least of $PC_{61}BM$ radical anion in case of X-, K-bands and probably Q-band LESR taking into account an overlap of ENDOR spectra around f_L via the strong contribution of both overlapped LESR spectra.

Additionally, the principal values of the g-tensors of $PC_{61}BM$ radical anion calculation also exhibits the slight difference between a- and aa-conformers and confirms the more suitable version of aa-conformer due to their more close values to experimental ones as shown in Table 1. The same calculation for the $(PPV\text{-}6)^+$ oligomer indicates a good agreement with the experimental g_i tensor values as well.

Table 1. Principal Values of the g-Tensors of $PC_{61}BM$ Radical Anion and PPV-6 Oligomer (Six Monomer Fragments) Cation Radical in P2:$PC_{61}BM$ Blend

	$(PC_{61}BM)^-$			P2	
		calculated (*-conformer*)			
G[a]	exptl[b]	*aa-*	*a-*	exptl[b]	calcd $(PPV\text{-}6)^+$
g_3	2.0004	2.00085	2.00086	2.0038	2.0042
g_2	2.0002	2.00057	2.00061	2.0027	2.0026
g_1	1.9986	1.99879	1.99888	2.0022	2.0023

[a]Numbering of the g_i tensor values follows the scheme employed by the ORCA program package, $g_3 > g_2 > g_1$. [b]In frozen *o*-DCB solution of P2:$PC_{61}BM$ blend at 20 K. The simulated spectrum is introduced in S4.

4. CONCLUSION

This study demonstrates the advantage of W-band multiresonance ^1H ENDOR/TRIPLE application to the system with small overlapping hfc values in ion radicals generated in OSC devices under the light excitation. The sign of proton hfcs obtained by TRIPLE allows the validation of the DFT data with essentially better accuracy that could be considered as an important point in the choice of isomers morphology as well as determination of polaron length delocalization along the conjugated polymer chain. With respect to the fullerene derivatives, the side chain protons can be considered as experimental spin label for spin density distribution of carbons atom on fullerene frame based on the appropriate data of its side chain via comparison of experiments and DFT. Therefore, W-band ENDOR/TRIPLE can be considered as one of the efficient experimental multiresonance methods suitable for the confirmation of the appropriate DFT data.

■ ASSOCIATED CONTENT

Supporting Information

The Supporting Information is available free of charge on the ACS Publications website at DOI: 10.1021/acs.jpcc.6b08034.

Additional information on the DFT calculation of PPV 5-,7-,8-oligomers, other version of PPV polaron ENDOR spectra fitting, and W-band $PC_{61}BM$ LESR spectrum simulation (PDF)

■ AUTHOR INFORMATION

Corresponding Author

*E-mail: alexander.konkin@tu-ilmenau.de. Phone: +49 03677 693437.

Notes

The authors declare no competing financial interest.

■ ACKNOWLEDGMENTS

Financial support from Deutsche Forschungsgemeinschaft (DFG) Project ID: RI966/11-1 is gratefully acknowledged. Author thanks D. A. M. Egbe for polymer supply.

■ REFERENCES

(1) Kaur, N.; Singh, M.; Pathak, D.; Wagner, T.; Nunzi, J. M. Organic Materials for Photovoltaic Applications: Review and Mechanism. *Synth. Met.* **2014**, *190*, 20−26.

(2) Niklas, J.; Mardis, K. L.; Banks, B. P.; Grooms, G. M.; Sperlich, A.; Dyakonov, V.; Beaupre, S.; Leclerc, M.; Xu, T.; Yu, L.; Poluektov, O. G. Highly-Efficient Charge Separation and Polaron Delocalization in Polymer−Fullerene Bulk-Heterojunctions: a Comparative Multi-Frequency EPR and DFT Study. *Phys. Chem. Chem. Phys.* **2013**, *15*, 9562−9574.

(3) Marumoto, K.; Kato, M.; Kondo, H.; Kuroda, S.; Greenham, N. C.; Friend, R. H.; Shimoi, Y.; Abe, S. Electron Spin Resonance and Electron Nuclear Double Resonance of Photogenerated Polarons in Polyfluorene and its Fullerene Composite. *Phys. Rev. B: Condens. Matter Mater. Phys.* **2009**, *79*, 245204−11.

(4) (a) Kuroda, S.; Noguchi, T.; Ohnishi, T. Electron Nuclear Double Resonance Observation of π- Electron Defect States in Undoped Poly(Paraphenylene Vinylene). *Phys. Rev. Lett.* **1994**, *72*, 286−289. (b) Kuroda, S.; Noguchi, T.; Ohnishi, T. ENDOR Spectroscopy of Poly (Paraphenylene Vinylene). *Synth. Met.* **1995**, *69*, 423−424. (c) Kuroda, S. ESR and ENDOR Studies of Solitons and Polarons in Conjugated Polymers. *Appl. Magn. Reson.* **2003**, *23*, 455−468.

(5) Aguirre, A.; Gast, P.; Orlinskii, S.; Akimoto, I.; Groenen, E. J. J.; El Mkami, H.; Goovaerts, E.; Van Doorslaer, S. Multifrequency EPR Analysis of the Positive Polaron in I_2-Doped Poly(3-Xylthiophene) and in Poly[2-Methoxy-5-(3,7-Dimethyloctyloxy)]-1,4-Phenylene Vinylene. *Phys. Chem. Chem. Phys.* **2008**, *10*, 7129−7138.

(6) Mardis, K. L.; Webb, J. N.; Holloway, T.; Niklas, J.; Poluektov, O. G. Electronic Structure of Fullerene Acceptors in Organic Bulk-Heterojunctions: A Combined EPR and DFT Study. *J. Phys. Chem. Lett.* **2015**, *6*, 4730−4735.

(7) Kietzke, T.; Egbe, D. A. M.; Hörhold, H.-H.; Neher, D. Comparative study of M3EH−PPV- based bilayer photovoltaic devices. *Macromolecules* **2006**, *39*, 4018−4022.

(8) Laikov, D. N.; Ustynyuk, Y. A. PRIRODA-04: A Quantum-Chemical Program Suite. New Possibilities in the Study of Molecular Systems With the Application of Parallel Computing. *Russ. Chem. Bull.* **2005**, *54*, 820−826.

(9) Laikov, D. N. Fast Evaluation of Density Functional Exchange-Correlation Terms Using the Expansion of the Electron Density in Auxiliary Basis Sets. *Chem. Phys. Lett.* **1997**, *281*, 151−156.

(10) Neese, F. The ORCA program system. *WIREs Comput. Mol. Sci.* **2012**, *2*, 73−78.

DOI: 10.1021/acs.jpcc.6b08034
J. Phys. Chem. C 2016, 120, 28905−28911

(11) Humphrey, W.; Dalke, A.; Schulten, K. VMD - Visual Molecular Dynamics. *J. Mol. Graphics* **1996**, *14*, 33−38.
(12) Deguchi, Y.; Okada, K.; Yamauchi, J. General Triple Resonance of Diphenyl Nitroxidede. *Chem. Lett.* **1983**, *12*, 1611−1614.
(13) Cook, R. J.; Whiffen, D. H. Relative Signs of Hyperfine Coupling Constants by a Double ENDOR Experiment. *Proc. Phys. Soc., London* **1964**, *84*, 845−848.
(14) Murphy, D. M.; Farley, R. D. Principles and Applications of ENDOR Spectroscopy for Structure Determination in Solution and Disordered Matrices. *Chem. Soc. Rev.* **2006**, *35*, 249−268.

DOI: 10.1021/acs.jpcc.6b08034
J. Phys. Chem. C 2016, 120, 28905−28911